Journal of Dental Research
2015, Vol. 94(3) 412–420

DOI: 10.1177/0022034514564186
jdr.sagepub.com

Amelogenins as Potential Buffers during Secretory-stage Amelogenesis

J. Guo[1], D.M. Lyaruu[1], Y. Takano[2], C.W. Gibson[3], P.K. DenBesten[4], and A.L.J.J. Bronckers[1]

Abstract

Amelogenins are the most abundant protein species in forming dental enamel, taken to regulate crystal shape and crystal growth. Unprotonated amelogenins can bind protons, suggesting that amelogenins could regulate the pH in enamel in situ. We hypothesized that without amelogenins the enamel would acidify unless ameloblasts were buffered by alternative ways. To investigate this, we measured the mineral and chloride content in incisor enamel of amelogenin-knockout (*AmelX*$^{-/-}$) mice and determined the pH of enamel by staining with methyl-red. Ameloblasts were immunostained for anion exchanger-2 (Ae2), a transmembrane pH regulator sensitive for acid that secretes bicarbonate in exchange for chloride. The enamel of *AmelX*$^{-/-}$ mice was 10-fold thinner, mineralized in the secretory stage 1.8-fold more than wild-type enamel and containing less chloride (suggesting more bicarbonate secretion). Enamel of *AmelX*$^{-/-}$ mice stained with methyl-red contained no acidic bands in the maturation stage as seen in wild-type enamel. Secretory ameloblasts of *AmelX*$^{-/-}$ mice, but not wild-type mice, were immunopositive for Ae2, and stained more intensely in the maturation stage compared with wild-type mice. Exposure of *AmelX*$^{-/-}$ mice to fluoride enhanced the mineral content in the secretory stage, lowered chloride, and intensified Ae2 immunostaining in the enamel organ in comparison with non-fluorotic mutant teeth. The results suggest that unprotonated amelogenins may regulate the pH of forming enamel in situ. Without amelogenins, Ae2 could compensate for the pH drop associated with crystal formation.

Keywords: pH control, enamel, SLC4A2, mineral density, dentin, alveolar bone

Introduction

Dental enamel is a unique biological tissue in that it is acellular, highly mineralized, and comprised of individual hydroxyapatite crystallites that are much longer and thicker than any other mineralized tissue (Simmer and Fincham 1995). Unlike collagen-based mineralized tissues such as dentin and bone, where mineralization occurs as a two-step process (secretion of a layer of organic matrix followed by mineralization of this matrix layer), enamel formation occurs as a gradual replacement of organic matrix with minerals (Simmer et al. 2010). In enamel, mineral deposition begins with the formation of thin ribbon-like crystals very near the apical plasma membrane of secretory ameloblasts in a newly secreted amelogenin-rich extracellular matrix. Unlike mineralizing connective tissues, enamel matrix is only temporarily present and is gradually broken down and removed from the enamel space as the matrix is replaced with minerals. This happens predominantly in the maturation stage as the crystals are expanding in width and thickness, which eventually gives rise to mature enamel composed of very large densely packed crystals (Nylen et al. 1963; Kerebel et al. 1979).

Amelogenins are specific proteins produced by ameloblasts, constituting 90% of the developing enamel matrix, and are essential for the development of a layer of enamel of normal thickness, architecture, and composition (Robinson et al. 1982). The mechanisms by which amelogenins direct crystal growth are not well understood. The general view is that amelogenins self-assemble into

[1]Department of Oral Cell Biology, Academic Centre for Dentistry Amsterdam (ACTA), University of Amsterdam and VU University Amsterdam, MOVE Research Institute, Amsterdam, the Netherlands
[2]Section of Biostructural Science, Graduate School of Medical and Dental Sciences, Tokyo Medical and Dental University, Tokyo, Japan
[3]Department of Anatomy and Cell Biology, University of Pennsylvania School of Dental Medicine, Philadelphia, PA, USA
[4]Department of Oral and Craniofacial Sciences, School of Dentistry, University of California in San Francisco, CA, USA

A supplemental appendix to this article is published electronically only at http://jdr.sagepub.com/supplemental.

Corresponding Author:
A.L.J.J. Bronckers, Department of Oral Cell Biology, ACTA, Vrije Universiteit, Gustav Mahlerlaan 3004, 1081 LA Amsterdam, the Netherlands.
Email: a.bronckers@acta.nl

nanospheres that control enamel crystallite size and orientation by preventing the lateral fusion of crystallites, thus controlling mineral accretion at the sides of the crystals. The nanoglobules are thought to do so by preferentially attaching to the lateral surfaces of the initial crystals, believed to be *crystalline* octacalcium phosphates (OCP) (Moradian-Oldak et al. 2000; Rauth et al. 2009). However, it was proposed recently that the initial long crystallite ribbons in the secretory stage consist not of crystalline but *amorphous* calcium phosphates (ACP) and that adsorption of amelogenins followed rather than induced the shapes of the crystals (Simmer et al. 2012). A second possible function of amelogenins is that they act as a buffer to neutralize the protons that are generated during crystal formation (Smith, 1998; Smith et al. 2005). In this respect, amelogenins contain 14 histidine residues, which bind protons, such that a single unprotonated amelogenin molecule can bind 11 to 15 protons per molecule in vitro (Ryu et al. 1998). In comparison, alpha-chymotrypsinogen A, a molecule of molecular weight similar to that of amelogenins but containing only 2 histidine residues/molecule, binds from 2.2 to 3.8 protons (Ryu et al. 1998).

In this study, we tested the hypothesis that amelogenins foster crystal formation by acting as space fillers between crystallites. Furthermore, we examined the role of amelogenins as a potential buffer for the local control of pH during crystal growth. Using *AmelX*$^{-/-}$ mice, we speculated that without being buffered by amelogenins, secretory-stage enamel would acidify more rapidly. This would influence the dynamics of crystal growth. It might also evoke a response of the ameloblasts to normalize pH by the secretion of bicarbonates, which normally occurs at the maturation stage (Smith et al. 2005; Lacruz et al. 2013). To further acidify the forming enamel, we exposed *AmelX*$^{-/-}$ mice to fluoride to induce the formation of hypermineralized lines, releasing more protons (Lyaruu et al. 1989; Lyaruu et al. 2014).

We investigated this by comparing the composition of developing enamel in 4 groups of mice. The first 2 groups were *AmelX*$^{-/-}$ mice given either 0 or 100 ppm fluoride in drinking water for 6 wk. The third and fourth groups were wild-type littermates treated identically. The mineral density was determined by microcomputed tomography (microCT), and the enamel composition by quantitative electron probe x-ray microanalysis (EPMA). Changes in pH in forming enamel were assessed by staining with methyl-red solution and immunolocalization of anion exchanger-2 (Ae2), a critical pH regulator in maturation ameloblasts (Bronckers et al. 2009; Lyaruu et al. 2014).

Materials and Methods

Animals, Tissues, and Tissue Processing

AmelX$^{-/-}$ mice were generated as reported previously (Gibson et al. 2001). The background of the wild-type mice is C57Bl/6, whereas the *AmelX*$^{-/-}$ mice are maintained in C56Bl/6 x 129/Sv. Twelve mice (21 d old) were examined in 4 groups of 3: wild-type and *AmelX*$^{-/-}$ mice, and wild-type and *AmelX*$^{-/-}$ mice exposed to 100 ppm fluoride for 6 wk. Animals were sacrificed, and mandibles and maxillae were quickly collected. From each group of 3 mice, one set of hemi-mandibles and hemi-maxillae was fixed by immersion in 5% paraformaldehyde in 0.1 M phosphate buffer plus 2% sucrose. After one series of hemi-mandibles from each group was scanned for microCT analysis, all jaws were decalcified in neutral ethylenediaminetetraacetic acid (EDTA), embedded in paraffin, and processed for immunohistochemical staining. The other hemi-mandibles from each group were slam-frozen in liquid nitrogen immediately after sacrifice, freeze-dried, and anhydrously embedded in methyl methacrylate (MMA) for EPMA. The freezedried mandibles of another 12 mice were used for pH staining. All procedures were approved by the Committee for Animal Health and Animal Care of the Vrije Universiteit and by the Institutional Animal Care and Use Committee of the University of Pennsylvania, USA.

MicroCT

Hemi-mandibles were scanned at a resolution of 6 μm voxels in a microCT-40 high-resolution scanner (Scanco Medical, AG, Bassersdorf, Switzerland) to measure mineral density in enamel, crown dentin, and surrounding alveolar bone. Beginning at the apical part of the incisor and moving toward the tip, cross-sectioned images through the incisors were collected at sequential intervals of 300 μm in maturation-stage and 60 μm in secretory-stage enamel. In each slice, the mineral density of enamel was measured halfway through the enamel layer at 3 sites within a circular area, with a diameter of 7 μm at the mesial, lateral, and central sides. Values of each tissue were averaged per slice. In wild-type mandibular incisors, enamel maturation begins approximately at the level where an imaginary line drawn between first and second molars intersects the incisor; in that area, the mineral density of secretory-stage enamel equals that of dentin (approximately 1,660 mg HA/cm^3 in this case), and the dentin layer is around 100 μm wide. Secretory-stage enamel in amelogenin-free incisors of *AmelX*$^{-/-}$ mice was identified by a combination of different landmarks, including the position of the forming incisor enamel in relation to molars, the mineral density of the adjacent dentin layer, and the thickness of the dentin layer in cross-sections. In *AmelX*$^{-/-}$ mice, the ''secretory'' ameloblasts also stained strongly with ameloblastin. For secretory-stage enamel of *AmelX*$^{-/-}$ mice, measurements were made apically from the area where the dentin layer was thinner than 100 μm wide and the dentin was less mineralized than 1,660 mg HA/cm^3. Mean values and standard deviation of the mineral density were calculated and presented as mean (SD). Differences in mineral density of dental tissues were evaluated by analysis of variance (ANOVA) ($P < 0.05$ as significant).

Electron Probe Microanalysis

Back-scattered electron detector microscopy and quantitative elemental analysis of enamel were carried out in cross-sections of MMA-embedded mouse mandibular incisors by EPMA at preeruptive stages at the level of the bone crest of the gingiva (gingival edge) with a Jeol Super Probe (JXA-8800; JEOL, Tokyo, Japan) (Lyaruu et al. 2014). Mean values and standard deviations of the content of CaO, F, Cl, and SO_3 in the enamel of each group were calculated and presented as weight percent. The differences in the enamel, dentin, and alveolar bone contents were evaluated by ANOVA ($P < 0.05$ as significant).

Staining with pH Indicator Methyl-red

Bone and enamel organ were rapidly micro-dissected from freeze-dried hemi-mandibles from 3 *AmelX*$^{-/-}$ and 3 wild-type mice. The exposed enamel surfaces in the hemi-mandibles were immersed for 3 min in 1 mg methyl red/ml, dissolved in distilled water containing 1 μMol NaOH, and blotted with filter paper, after which micrographs were taken (Lyaruu et al. 2014).

Immunohistochemistry

EDTA-decalcified, paraffin-embedded tissue sections were immunostained with rabbit anti-ameloblastin serum (1:1000; courtesy Dr. Uchida, Japan; Lee et al. 1996), rabbit anti-porcine amelogenin (1:2,000; Uchida et al. 1991), rabbit anti-mouse antiserum (1:800, courtesy Dr. J. Simmer, Michigan, USA), or rabbit anti-Ae2 (1:50; courtesy Dr. S. Kellokumpu, University of Oulu, Finland). Dewaxed and rehydrated paraffin sections were washed in Tris-buffered saline (TBS). Anti-Ae2 staining required retrieval in 10 mM citrate buffer (pH 6.0) overnight at 60ºC (Bronckers et al. 2009). Staining in extracellular enamel matrix with anti-porcine amelogenins sections required retrieval in 0.5 mM EGTA in 10-mM Tris (pH 9.0) at 60°C for 5 h. Endogenous peroxidase was inactivated by 5-minute incubation in Dual Endogenous Enzyme Block (EnVision kit, DakoCytomation, Glostrup, Denmark), then washed in TBS and blocked with normal goat sera. Sections were incubated with primary antibodies, non-immune rabbit IgG, or normal rabbit serum (negative controls) overnight at 4ºC, rinsed, and incubated with secondary antibody, goat anti-rabbit peroxidase conjugate (EnVision kit, DakoCytomation), or goat anti-rabbit FITC conjugate (SantaCruz Biotec, Dallas, TX, USA) for 1 h at ambient temperature. Peroxidase activity was visualized by DAB (EnVision kit), counterstained with aqueous hematoxylin, dehydrated through a gradient series of alcohols, and mounted in Depex or Vectashield (immunofluorescence; Vector Labs, Burlingame, CA, USA).

Results

Mineral Density of Enamel is Substantially Changed during Enamel Development in AmelX$^{-/-}$ Mice

In the mandibular incisors of *AmelX*$^{-/-}$ mice, the enamel thickness was approximately 10% of that in wild-type mice. Disruption of the amelogenin gene substantially changed the normal pattern of mineralization in enamel, but not dentin or surrounding bone (Appendix Fig. a, b). In the secretory-stage enamel of *AmelX*$^{-/-}$ mice, mineralization began earlier, and mineral density at similar stages reached higher values than did secretory-stage enamel of wild-type mice (Figs. 1a, b). In secretory-stage enamel of *AmelX*$^{-/-}$ mice, mineral density was, on average, 1.8-fold higher [1,445 ± 84 mg hydroxyapatite (HA)/cm^3] than in wild-type controls (796 ± 92 mg HA/cm^3) (Fig. 1a; Table). In the maturation stage, however, mineral accretion in *AmelX*$^{-/-}$ enamel lagged behind and reached a value 0.73-fold of that in wild-type incisors (1,916 ± 66 mg HA/cm^3 in *AmelX*$^{-/-}$ mice vs. 2,611 ± 45 mg HA/cm^3 in wild-type mice; Fig. 1c; Table). Final mineral density of maturation-stage enamel in *AmelX*$^{-/-}$ mice was comparable with that of dentin (1,745 ± 3 mg HA/cm^3) (Fig. 1c, Appendix Fig. b).

Exposure to Fluoride Increased Mineral Density in the Secretory Stage of AmelX$^{-/-}$ Enamel but Decreased It in the Secretory Stage of Wild-type Enamel

Exposure of wild-type mice to fluoride reduced the mineral density of secretory-stage enamel by 0.78-fold of control values (not statistically significant) and by 0.46-fold in maturation-stage enamel ($P < 0.001$, Fig. 1c; Table). In contrast, in *AmelX*$^{-/-}$ mice, exposure to fluoride increased mineral density 1.13-fold in the secretory stage ($0.01 < P < 0.05$) and 1.05-fold (not statistically significant) in the maturation stage (Fig. 1c; Table). Hence, the effect of fluoride on the mineral density in enamel of *AmelX*$^{-/-}$ mice was 2.6-fold more potent in the secretory stage and 1.7-fold more potent in the maturation stage compared with that in wild-type enamel ($P < 0.001$, Table). Mineral density in the dentin of *AmelX*$^{-/-}$ mice was slightly lower than that in wild-type mice, while alveolar bone mineral density was not influenced (Fig. 1c).

Back-scattered electron detector microscopy revealed that fluorotic maturation-stage enamel in wild-type mice was heterogeneous. Most enamel was hypomineralized, with thin hyper-mineralized layers at the surface and in the inner layer of enamel (Fig. 2a, b). The much thinner enamel in *AmelX*$^{-/-}$ mice showed a heterogeneously mineralized surface layer, hypomineralized subsurface, and hypermineralized layers in deeper enamel (Figs. 2c, d).

Electron Probe Microanalysis (EPMA) of Enamel Composition at the Late-maturation Stage

Calcium content in maturation-stage enamel was lower in *AmelX*$^{-/-}$ mice than in wild-type controls, but was the same for dentin and bone (Fig. 2e). Fluoride reduced the calcium content of maturation-stage enamel in wild-type but not in *AmelX*$^{-/-}$ mice (Fig. 2e).

There was no difference in the fluoride content in enamel of unexposed wild-type mice and *AmelX*$^{-/-}$ mice, and levels were similar to those in dentin (Fig. 2f). Significantly higher levels of fluoride were measured in all fluorotic tissues in both wild-type and *AmelX*$^{-/-}$ mice, with a larger increase in alveolar bone (Fig. 2f).

In *AmelX*$^{-/-}$ enamel, the chloride (Fig. 2g) and calcium levels (Fig. 2e) were lower than in wild-type mice, an effect also apparent in fluorotic wild-type enamel (Fig. 2g). In fluorotic *AmelX*$^{-/-}$ enamel, chloride was further reduced and reached the lowest values of all groups (Fig. 2g).

Sulfur trioxide (SO_3) content (representing matrix proteins with sulfur-containing amino acids) in the late maturation stage remained highest in fluorotic wild-type enamel, less in fluorotic and non-fluorotic amelogenin-free enamel, and was lowest in wild-type enamel (Fig. 2h).

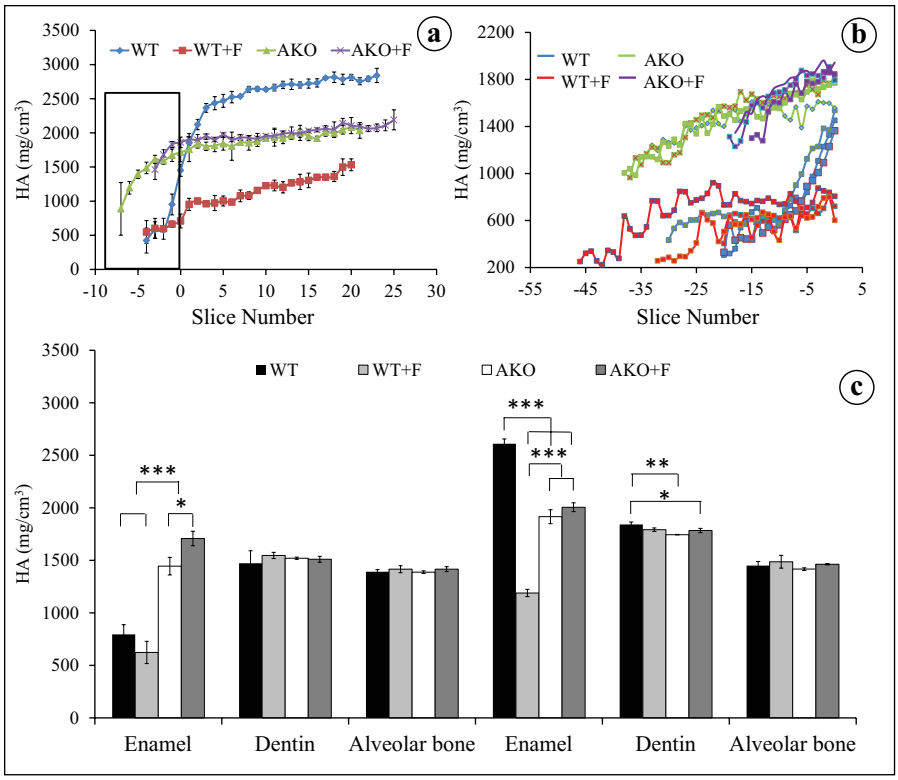

Figure 1. The mineral density of lower incisor enamel from unexposed and fluoride (F)-exposed *AmelX*$^{-/-}$ mice measured by micro CT. (**a, b**) The density in the 4 groups was plotted against slice numbers (representing progressive stages of enamel formation with 300 µm intervals for (a), or 60 µm intervals for (b)). 0 in the X axis stands for the beginning of the maturation stage. Negative numbers along X axis represent the secretory stage. The boxed area (secretory stage) in (a) is shown in more detail in (b). In (b) the graphs with the same color (blue, red, green, or purple) represent measurements of separate mice from the same experimental group. (c) The average values of secretion-stage and maturation-stage enamel in comparison with the values for dentin and bone are shown for each group. WT, wild-type mice; WT+F, wild-type mice exposed to fluoride; AKO, *AmelX*$^{-/-}$ mice; AKO+F, *AmelX*$^{-/-}$ mice exposed to fluoride. Exposure of wild-type mice and *AmelX*$^{-/-}$ mice to fluoride had opposite effects on the enamel mineral density. ***$P < 0.001$; **$0.001 < P < 0.01$; *$0.01 < P < 0.05$.

Secretory ameloblasts of wild-type mice (Fig. 3a), but not *AmelX*$^{-/-}$ mice (Fig. 3b), stained strongly for amelogenin. Secretory ameloblasts of both wild-type mice (Fig. 3c) and *AmelX*$^{-/-}$ mice (Fig. 3d) stained strongly for ameloblastin. Whereas in wild-type incisors, extracellular staining for amelogenin disappeared at mid-maturation (Fig. 3e), in fluorotic wild-type incisors, strong staining for amelogenins was retained from the early secretory stage until eruption (Fig. 3f).

AmelX$^{-/-}$ *Enamel Stained with Methyl-red*

In wild-type mice, secretory-stage enamel stained neutral with methyl-red. In maturation-stage enamel, methyl-red staining revealed 2 broad acidic bands (Fig. 4a), the first intensely deep-red and the second (incisal) much weaker. No such red bands were noted in the enamel of *AmelX*$^{-/-}$ mice (Fig. 4b).

In AmelX$^{-/-}$ *Mice, Secretory Ameloblasts Expressed Ae2*

In *AmelX*$^{-/-}$ mice, secretory ameloblasts were positive for Ae2 (Fig. 4c). This staining was weak at the early secretory stage, increased at the mid-secretory stage, and was intense at the maturation stage (Fig. 4c, f, h, j). Also, the stratum intermedium and papillary layer strongly reacted with anti-Ae2 (Fig. 4f, h, j). In wild-type mice, however, Ae2 immunostaining was restricted to the layer of maturation ameloblasts and was less intense than in null-mutant cells (Fig. 4d, e, g, i).

Exposure of *AmelX*$^{-/-}$ mice to fluoride markedly enhanced staining intensity for Ae2 (Fig. 4k, l).

Table. Changes in Mineral Density of Forming Enamel in the Absence of Amelogenins with or without Exposure to Fluoride (proportional as treatment/control).

	Mineral Density in Extracellular Enamel			
	Effect of *AmelX*$^{-/-}$ [a]	Effect of F on wild-type mice[b]	Effect of F on *AmelX*$^{-/-}$ [c]	Effect of *AmelX*$^{-/-}$ on F potency[d]
Secretion	1.82***	0.78	1.13*	2.62***
Maturation	0.73***	0.46***	1.05	1.69***

[a]*AmelX*$^{-/-}$ /WT.
[b]Fluorotic WT/WT.
[c]Fluorotic *AmelX*$^{-/-}$/*AmelX*$^{-/-}$.
[d]Fluorotic *AmelX*$^{-/-}$/fluorotic WT.
***$P < 0.001$. **$0.001 < P < 0.01$. *$0.01 < P < 0.05$.

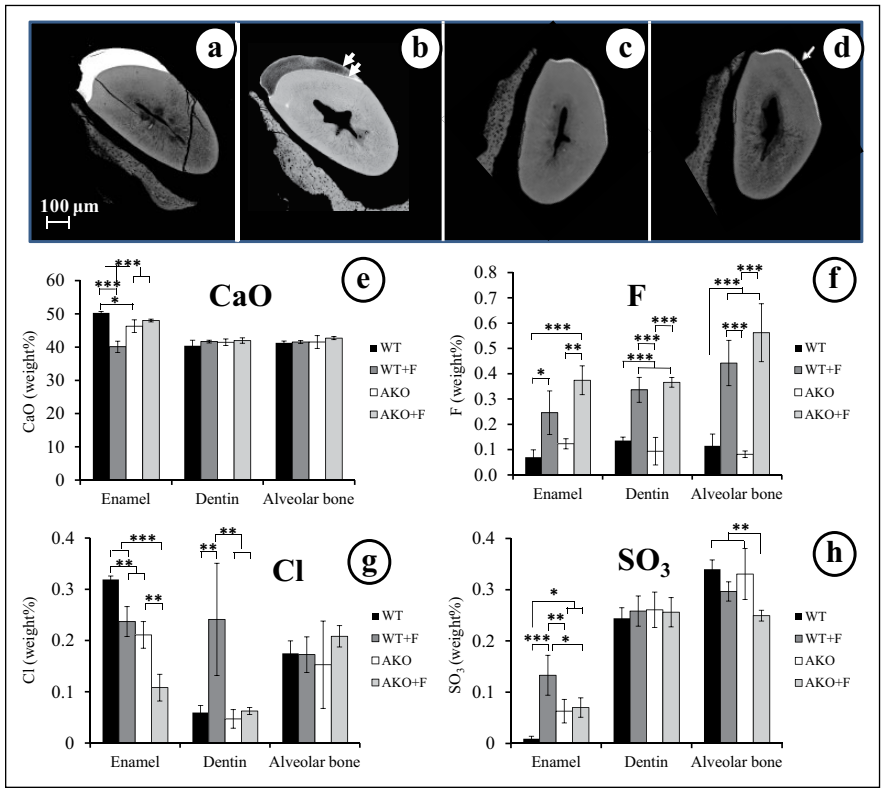

Figure 2. Backscattered (BSD) images and the composition of the enamel in late maturation-stage for different experimental groups measured by electron probe X-ray microanalysis (means and standard deviation). Late maturation enamel from wild-type (**a**), fluorotic wild-type (**b**), *AmelX*$^{-/-}$ (**c**) and fluorotic *AmelX*$^{-/-}$ (**d**) mandibular incisors. Disruption of amelogenin gene significantly reduced the enamel thickness (c, d). The white arrows in (b) show the hypermineralized lines in the superficial and deep fluorotic enamel layers. The white arrow in (d) shows the heterogeneous surface of the fluorotic *AmelX*$^{-/-}$ enamel. To highlight the changes in the enamel layer, the BSD images are presented with different dentin "densities." CaO (**e**), fluoride (**f**), chlorine (**g**) and SO3 (**h**). ***$P < 0.001$; **$0.001 < P < 0.01$; *$0.01 < P < 0.05$. WT, wild-type mice; WT+F: wild-type mice exposed to fluoride; AKO, *AmelX*$^{-/-}$ mice; AKO+F, *AmelX*$^{-/-}$ mice exposed to fluoride.

Discussion

Amelogenins as Potential Buffer in Secretory-stage Enamel

The histidine residues of amelogenins can bind from 11 to 15 protons per molecule in vitro (Ryu et al. 1998), suggesting that parent amelogenins have the potential to act as a buffer to neutralize protons. Formation of apatites releases protons, a process that is accelerated at slightly acidic pH and in the presence of fluoride. Wild-type secretory-stage enamel is pH-neutral (Smith 1998), and secretory ameloblasts do not express basolateral Ae2 (Lyaruu et al. 2008; Bronckers et al. 2009). When the rate of mineral deposition increases after the transitional stage, ameloblasts begin to express Ae2 in their basolateral membranes, a known transmembrane protein involved in pH regulation (Lyaruu et al. 2008; Alper 2009; Concepcion et al. 2014). The positive staining for Ae2 in secretory ameloblasts lining more strongly mineralized enamel in *AmelX*$^{-/-}$ mice suggests that, in the absence of amelogenins, secretory ameloblasts begin to express Ae2 to compensate for the lack of buffering.

It should be noted that analysis of our data does not prove that amelogenins buffer protons in situ, though this explanation is likely. We compared the mineral density of secretory-stage wild-type enamel with that in amelogenin-deficient enamel at the same position, the (anatomical) distance from the onset of enamel mineralization. A better way would have been to calculate and compare the mineral density for the same volume of enamel (normalized per cell or matrix), which takes into account that, in null mice, the enamel layer is much thinner than in wild-type enamel. Accurate volume measurement of freeze-dried early-secretory enamel in microCT images, however, was not possible.

How Ae2 in ameloblasts is upregulated in the absence of amelogenins is unknown. One possibility is that ameloblasts respond to the acidification of enamel by upregulating Ae2. In Xenopus oocytes transfected with Ae2 (Humphreys et al. 1994) and in mouse LS2 ameloblast-like cell line cultures, Ae2 expression is sensitive for and responds to intra- and extracellular pH changes with a maximum expression at pH 6.8 (Paine et al. 2008). In vivo chronic metabolic acidosis enhances Ae2 protein levels 6-fold in the renal cortex of rats, while metabolic alkalosis reduces Ae2 protein levels by 50% (Quentin et al. 2004). Alternatively, the upregulation of Ae2 in *AmelX*$^{-/-}$ mice could be explained by the absence of amelogenins per se, which could change the production of other proteins. Except for a small increase in ameloblastin expression (Lu et al. 2011), there are no published reports of changes in expression patterns in amelogenin-deficient ameloblasts. In wild-type rodents, amelogenins and amelogenin fragments have been detected at low levels in bone cells, odontoblasts, cementocytes, and soft tissues (Deutsch et al. 2006; Haruyama et al. 2011; Jacques et al. 2014) and have been proposed to act as signaling factors that bind to intracellular or extracellular receptors (Chen et al. 2011; Haruyama et al. 2011; Jacques et al. 2014). Such signaling may not happen in the ameloblasts of *AmelX*$^{-/-}$ mice, which could change the normal development of ameloblasts, resulting in a premature transformation of ameloblasts into maturation-like cells.

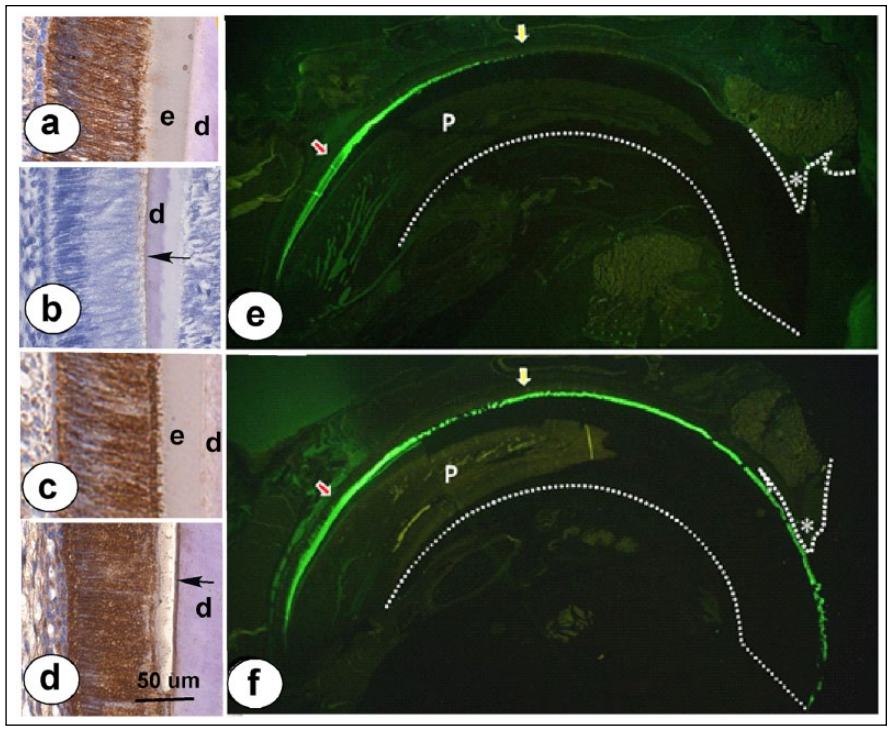

Figure 3. Immunolocalization of amelogenin (**a, b, e, f**) and ameloblastin (**c, d**) in developing maxillary incisors. Secretory ameloblasts of wild-type mice are positive for amelogenin (a) and ameloblastin (c). Ameloblasts of *AmelX*$^{-/-}$ mice are negative for amelogenin (b) but strongly positive for ameloblastin (d). Arrows point to the thin layer of enamel in null mice. In upper incisors of wild-type mice, amelogenin disappears by the mid-stage of maturation (e, yellow arrow), whereas intense amelogenin immunoreactions persist throughout the maturing and post-eruptive enamel layers in fluorotic wild-type incisors (f). a, b, rabbit anti-mouse amelogenins; e, f, rabbit anti-porcine amelogenins. Red arrows indicate transitional stage. P, dental pulp; *gingival margin; d, dentin; e, enamel.

Absence of Amelogenins Reduces Crystal Dimensions by a Lack of Crystal Fostering and pH Regulation

The dimensions of the fully matured enamel crystals in *AmelX*$^{-/-}$ enamel have been reported to be significantly smaller than in wild-type enamel. In erupted first molars of *AmelX*$^{-/-}$ mice, crystals were 59 ± 11 nm wide and 16 ± 4 nm thick, whereas in wild-type mice, crystals were 96 ± 14 nm wide and 25 ± 5 nm thick (Wright et al. 2011). Amelogenins have been shown *in vivo* to form nanosphere aggregates (Fincham et al. 1995) and aggregate into higher-order structures that regulate the rate and size of crystal formation (Moradian-Oldak et al. 1995; Moradian-Oldak 2013). The sizes and formation of nanoglobules depend on the local pH, and aggregates will disaggregate at low pH, thereby losing control of crystal growth (Moradian-Oldak and Goldberg 2005; Margolis et al. 2006). The fact that enamel crystallites in *AmelX*$^{-/-}$ enamel are smaller than in wild-type enamel (Wright et al. 2011) supports the concept that, by tightly controlling pH near the crystal surfaces, amelogenins could regulate their own aggregation, disaggregation, and conformation and hence control the shapes and final dimensions of the enamel crystallites. Without amelogenins, ameloblasts lose control over regulating the kinetics of crystal growth. This could potentially give rise to the thinner, smaller, and likely shorter crystals in *AmelX*$^{-/-}$ enamel that resemble the (small) crystals formed in dentin and bone.

Analysis of our EPMA and immunohistochemical data showed that there was significantly more matrix remaining in fluorotic and *AmelX*$^{-/-}$ enamel than in wild-type enamel. The matrix in *AmelX*$^{-/-}$ consisted of non-amelogenins

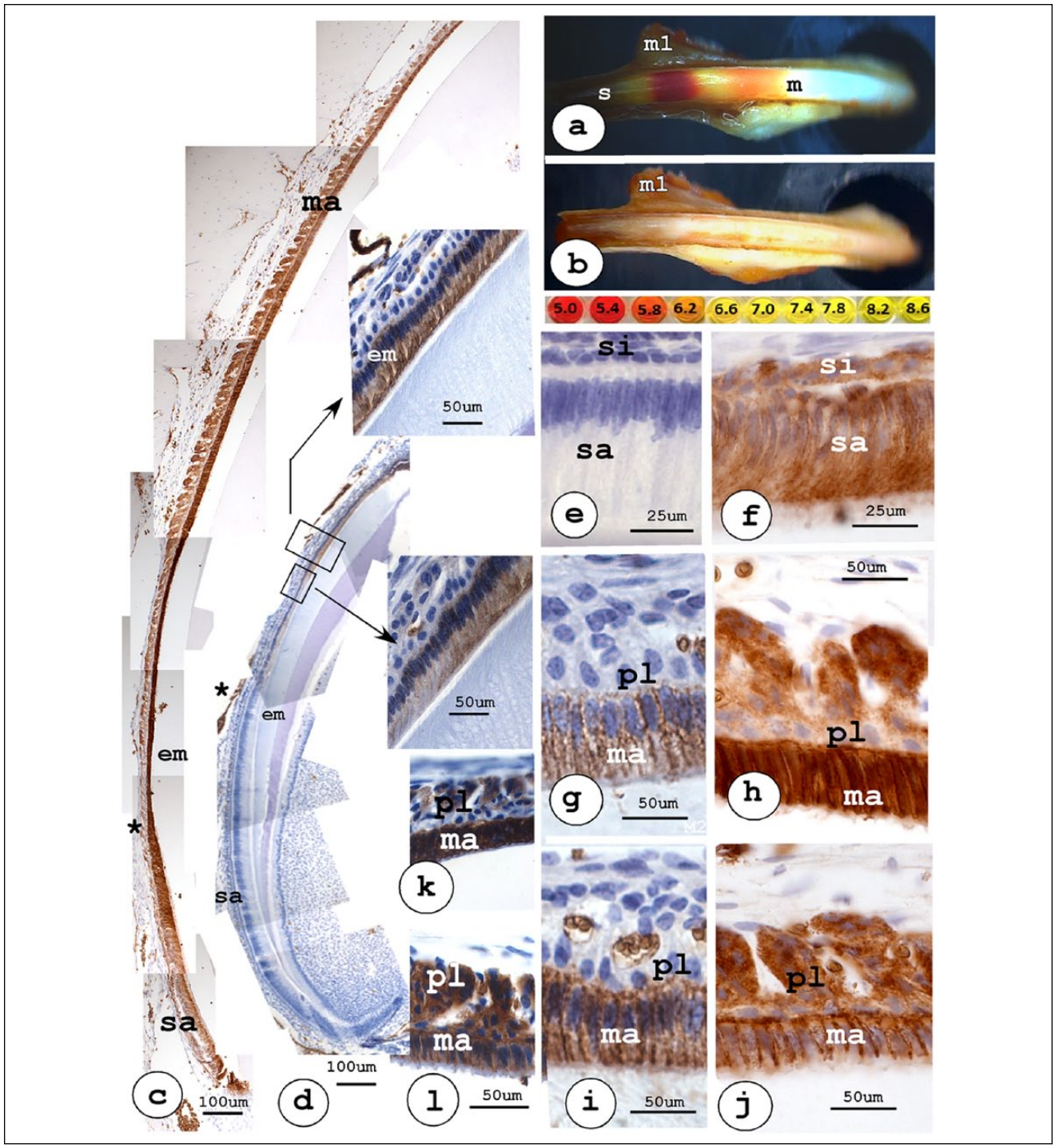

Figure 4. Staining for pH (**a, b**) and Ae2 protein (**c–l**) during amelogenesis in incisors from *AmelX*$^{-/-}$ mice and wild-type mice. (a) Methyl-red-stained cell-free enamel of lower incisors from a wild-type mouse and (b) from an *AmelX*$^{-/-}$ mouse. Methyl-red revealed 2 acidic bands, a dark-red one apically and a weaker pink (acidic) one more incisally in wild-type but not in *AmelX*$^{-/-}$ enamel. M1 indicates the position of the first molar. (c) A low-power micrograph of Ae2 immunostaining in upper incisors of a non-fluorotic *AmelX*$^{-/-}$ enamel organ. Ameloblasts, stratum intermedium (si), and papillary layer (pl) are strongly positive (f, h, j). In wild-type mouse incisors (d), staining for Ae2 is absent in secretory ameloblasts (sa) and gradually begins at early maturation, but staining is weaker. Boxed areas are magnified and restricted to maturation ameloblasts (ma; e, g, i). Asterisks in (c) and (d) indicate approximate onset of transitional stage. Exposure to fluoride strongly enhanced staining in fluorotic *AmelX*$^{-/-}$ enamel organ in early (k) and late maturation (l).

(methionine-containing ameloblastins and enamelins), compacted in a much thinner layer of enamel than in wild-type controls. In addition, disruption of *AmelX*$^{-/-}$ increased ameloblastin levels (Lu et al. 2011). Given the very thin layer of enamel in *AmelX*$^{-/-}$ mice in comparison with the spot size of our beam (7-micrometer diameter), some contribution of sulfur-containing components originating from dentin cannot be completely ruled out.

Thus, in amelogenin-deficient enamel, crystal growth is accelerated in the secretory stage, Ae2 is prematurely expressed, and the formation of acidic bands in maturation-stage enamel is impaired.

Author Contributions

J. Guo, contributed to design, data acquisition, analysis, and interpretation, drafted and critically revised the manuscript; D.M. Lyaruu, contributed to conception, design, data acquisition, analysis, and interpretation, critically revised the manuscript; Y. Takano, contributed to design, data acquisition, and analysis, drafted and critically revised the manuscript; C.W. Gibson, contributed to design, data analysis, and interpretation; critically revised the manuscript; P.K. DenBesten, contributed to conception, design, and data acquisition, critically revised the manuscript; A.L.J.J. Bronckers, contributed to conception, design, data analysis, and interpretation drafted and critically revised the manuscript. All authors gave final approval and agree to be accountable for all aspects of the work.

Acknowledgments

We thank Drs. Y. Li (Anatomy and Cell Biology, University of Pennsylvania, Philadelphia, USA) and Y. Nakano (Oral Sciences, University of San Francisco, CA, USA) for help in providing mutant mice; Drs. S. Kellokumpu (Biochemistry, University of Oulu, Finland), T. Uchida (Oral Biology, Hiroshima University, Japan), and J. Simmer (Biological and Material Sciences, University of Michigan, Ann Arbor, USA) for donating antibodies; Dr. A. Kulkarni (NIDCR NIH Bethesda, MA, USA) for his help in creating the amelogenin-null mouse strain; and Mr. W. Lustenhouwer and Dr. Sergei Matveev (VU University Amsterdam) for assistance with the microprobe determinations. The authors acknowledge the assistance of Mr. T.J.M. Bervoets (Oral Cell Biology ACTA) and Dr. L. van Ruijven (Functional Anatomy ACTA) for technical support, data acquisition, and interpretation. This study was supported by National Institutes of Health (NIH) DE13508, NIH DE019629, DE011089, and JSPS 24390408. The authors declare no potential conflicts of interest with respect to the authorship and/or publication of this article.

References

Alper SL. 2009. Molecular physiology and genetics of Na+-independent SLC4 anion exchangers. J Exp Biol. 212 (Pt 11):1672–1683.

Bronckers AL, Lyaruu DM, Jansen ID, Medina JF, Kellokumpu S, Hoeben KA, Gawenis LR, Oude-Elferink RP, Everts V. 2009. Localization and function of the anion exchanger Ae2 in developing teeth and orofacial bone in rodents. J Exp Zool B Mol Dev Evol. 312B(4):375–387.

Chen X, Li Y, Alawi F, Bouchard JR, Kulkarni AB, Gibson CW. 2011. An amelogenin mutation leads to disruption of the odontogenic apparatus and aberrant expression of Notch1. J Oral Pathol Med. 40(3):235–242.

Concepcion AR, Lopez M, Ardura-Fabregat A, Medina JF. 2014. Role of AE2 for pHi regulation in biliary epithelial cells. Front Physiol. 4:413.

Deutsch D, Haze-Filderman A, Blumenfeld A, Dafni L, Leiser Y, Shay B, Gruenbaum-Cohen Y, Rosenfeld E, Fermon E, Zimmermann B, et al. 2006. Amelogenin, a major structural protein in mineralizing enamel, is also expressed in soft tissues: brain and cells of the hematopoietic system. Eur J Oral Sci. 114(Suppl 1):183–189.

Fincham AG, Moradian-Oldak J, Diekwisch TG, Lyaruu DM, Wright JT, Bringas P Jr, Slavkin HC. 1995. Evidence for amelogenin "nanospheres" as functional components of secretory-stage enamel matrix. J Struct Biol. 115(1):50–59.

Gibson CW, Yuan ZA, Hall B, Longenecker G, Chen E, Thyagarajan T, Sreenath T, Wright JT, Decker S, Piddington R, et al. 2001. Amelogenin-deficient mice display an amelogenesis imperfecta phenotype. J Biol Chem. 276(34):31871–31875.

Haruyama N, Hatakeyama J, Moriyama K, Kulkarni AB. 2011. Amelogenins: multi-functional enamel matrix proteins and their binding partners. J Oral Biosci. 53(3):257–266.

Humphreys BD, Jiang L, Chermova MN, Alper SL. 1994. Functional characterization and regulation by pH of murine AE2 anion exchanger expressed in Xenopus oocytes. Am J Physiol Cell Physiol. 267:C1295–C1307.

Jacques J, Hotton D, De la Dure-Molla M, Petit S, Asselin A, Kulkarni AB, Gibson CW, Brookes SJ, Berdal A, Isaac J. 2014. Tracking endogenous amelogenin and ameloblastin in vivo. PloS One. 9(6):e99626.

Kerebel B, Daculsi G, Kerebel LM. 1979. Ultrastructural studies of enamel crystallites. J Dent Res. 58 (Spec Issue B):844–851.

Lacruz RS, Smith CE, Kurtz I, Hubbard MJ, Paine ML. 2013. New paradigms on the transport functions of maturation-stage ameloblasts. J Dent Res. 92(2):122–129.

Lee SK, Krebsbach PH, Matsuki Y, Nanci A, Yamada KM, Yamada Y. 1996. Ameloblastin expression in rat incisors and human tooth germs. Int J Dev Biol. 40(6):1141–1150.

Lu X, Ito Y, Kulkarni A. Gibson C, Luan X, Diekwisch TG. 2011. Ameloblastin-rich enamel matrix favors short and randomly oriented apatite crystals. Eur J Oral Sci. 119(Suppl 1):254–260.

Lyaruu DM, Blijleven N, Hoeben-Schornagel K, Bronckers AL, Woltgens JH. 1989. X-ray micro-analysis of the mineralization patterns in developing enamel in hamster tooth germs exposed to fluoride in vitro during the secretory phase of amelogenesis. Adv Dent Res. 3(2):211–218.

Lyaruu DM, Bronckers AL, Mulder L, Mardones P, Medina JF, Kellokumpu S, Oude Elferink RP, Everts V. 2007. The anion exchanger Ae2 is required for enamel maturation in mouse teeth. Matrix Biol. 27(2):119–127.

Lyaruu DM, Medina JF, Sarvide S, Bervoets TJ, Everts V, DenBesten P, Smith CE, Bronckers AL. 2014. Barrier formation: potential molecular mechanism of enamel fluorosis. J Dent Res. 93(1):96–102.

Margolis HC, Beniash E, Fowler CE. 2006. Role of macromolecular assembly of enamel matrix proteins in enamel formation. J Dent Res. 85(9):775–793.

Moradian-Oldak J. 2013. Protein mediated enamel mineralization. Front Biosci (Landmark Ed). 17:1996–2023.

Moradian-Oldak J, Goldberg M. 2005. Amelogenin supra-molecular assembly in vitro compared with the architecture of the forming enamel matrix. Cells Tissues Organs. 181(3-4):202–218.

Moradian-Oldak J, Simmer JP, Lau EC, Diekwisch T, Slavkin HC, Fincham AG. 1995. A review of the aggregation properties of a recombinant amelogenin. Connect Tissue Res. 32(1-4):125–130.

Moradian-Oldak J, Paine ML, Lei YP, Fincham AG, Snead ML. 2000. Self-assembly properties of recombinant engineered amelogenin proteins analyzed by dynamic light scattering and atomic force microscopy. J Struct Biol. 131(1):27–37.

Nylen MU, Eanes ED, Omnell KA. 1963. Crystal growth in rat enamel. J Cell Biol. 18:109–123.

Paine ML, Snead ML, Wang HJ, Abuladze N, Pushkin A, Liu W, Kao LY, Wall SM, Kim YH, Kurtz I. 2008. Role of NBCe1 and AE2 in secretory ameloblasts. J Dent Res. 87(4):391–395.

Quentin F, Eladari D, Frische S, Cambillau M, Nielsen S, Alper S, Paillard M, Chambrey R. 2004. Regulation of the Cl-/HCO3- exchanger AE2 in rat thick ascending limb of Henle's loop in response to changes in acid-base sodium balance. J Am Soc Nephrol. 15(12):2988–2997.

Rauth RJ, Potter KS, Ngan AY, Saad DM, Mehr R, Luong VQ, Schuetter VL, Miklus VG, Chang P, Paine ML, et al. 2009. Dental enamel: genes define biomechanics. J Calif Dent Assoc. 37(12):863–868.

Robinson C, Kirkham J, Briggs HD, Atkinson PJ. 1982. Enamel proteins: from secretion to maturation. J Dent Res. 61(Spec Iss):1490–1495.

Ryu OH, Hu CC, Simmer JP. 1998. Biochemical characterization of recombinant mouse amelogenins: protein quantitation, proton absorption, and relative affinity for enamel crystals. Connect Tissue Res. 38(1-4):207–214.

Simmer JP, Fincham AG (1995). Molecular mechanisms of dental enamel formation. Crit Rev Oral Biol Med. 6(2):84–108.

Simmer JP, Papagerakis P, Smith CE, Fisher DC, Rountrey AN, Zheng L, Hu JC. 2010. Regulation of dental enamel shape and hardness. J Dent Res. 89(10):1024–1038.

Simmer JP, Richardson AS, Hu YY, Smith CE, Hu JCC. 2012. A post-classical theory of enamel biomineralization… and why we need one. Int J Oral Sci. 4(3):129–134.

Smith CE. 1998. Cellular and chemical events during enamel maturation. Crit Rev Oral Biol Med. 9(2):128–161.

Smith CE, Chong DL, Bartlett JD, Margolis HC. 2005. Mineral acquisition rates in developing enamel on maxillary and mandibular incisors of rats and mice: implications to extracellular acid loading as apatite crystals mature. J Bone Miner Res. 20(2):240–249.

Uchida T, Tanabe T, Fukae M, Shimizu M, Yamada M, Miake K, Kobayashi S. 1991. Immunochemical and immunohistochemical studies, using antisera against porcine 25 kDa amelogenin, 89 kDa enamelin and the 13-17 kDa nonamelogenins, on immature enamel of the pig and rat. Histochemistry. 96(2):129–138.

Wright JT, Li Y, Suggs C, Kuehl MA, Kulkarni AB, Gibson CW. 2011. The role of amelogenin during enamel-crystallite growth and organization in vivo. Eur J Oral Sci. 119(Suppl 1):65–69.